CHALMERS
UNIVERSITY OF TECHNOLOGY

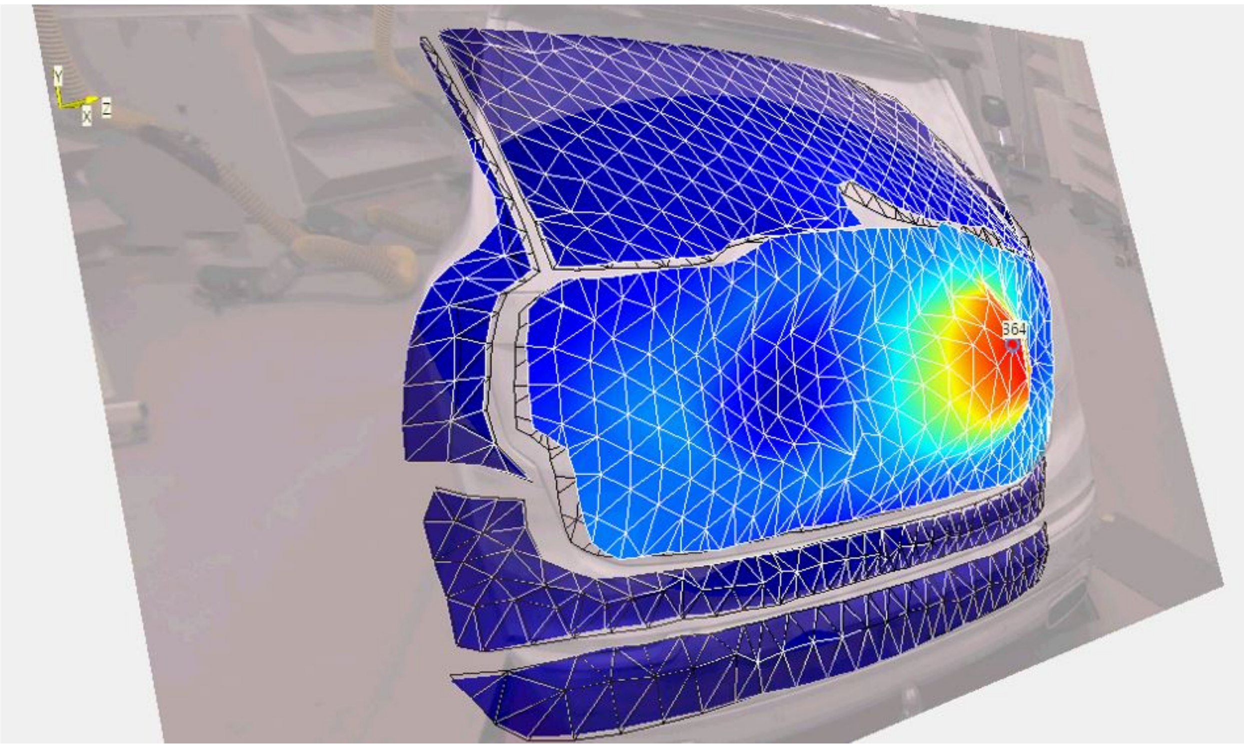

# *Experimental Study of Low-Mid Frequency Interior Noise of an SUV*

*Master's thesis in the Master's programme in Sound and Vibration*

*NAVEEN SADANANDA*

Department of Applied Mechanics
Division of Vehicle Engineering Autonomous Systems
CHALMERS UNIVERSITY OF TECHNOLOGY
Gothenburg, Sweden 2016

Master's thesis 2016:64

# Experimental Study of Low-Mid Frequency Interior Noise of an SUV

*NAVEEN SADANANDA*

CHALMERS
UNIVERSITY OF TECHNOLOGY

Department of Applied Mechanics
Division of Vehicle Engineering Autonomous Systems
Chalmers University of Technology
Gothenburg, Sweden 2016

**Experimental Study of Low-Mid Frequency Interior Noise of an SUV**
NAVEEN SADANANDA



Master's Thesis 2016:64
Department of Applied Mechanics
Division of Vehicle Engineering Autonomous Systems
Chalmers University of Technology
SE-412 96 Gothenburg
Telephone +46 (0)31 772 1000

Cover: Picture taken from Laser Doppler Vibrometer measurements.

Chalmers Reproservice
Gothenburg, Sweden 2016

Experimental Study of Low-Mid Frequency Interior Noise of an SUV

Master's thesis in the Master's programme in Sound and Vibration
NAVEEN SADANANDA
Department of Applied Mechanics
Division of Vehicle Engineering Autonomous Systems
Chalmers University of Technology

# Abstract

The reduction of wind noise of vehicle is important, mostly in the premium vehicle segment, in which the occupants are susceptible to the background noise inside the car. The elevated wind noise levels lead to discomfort and fatigue of the occupants in the car. It is hence a primary task that any windnoise concerns are analysed and resolved in the initial stages.

A 3D spherical beamforming array is a effective tool for localising sound sources inside the vehicle. When performing wind noise measurements in the tunnel, it is important to acquire as much information as possible efficiently, since the facility time is usually costly. With the limited measurement time available, the spherical beamforming tool allows the localisation of the important acoustic sources. Thus, different configurations with geometry modifications can be tested to assisit the test engineers to the optimum configurations and improve the efficiency of measurements.

The investigation involves characterisation of sound sources inside the vehicle caused by structural excitation due to turbulent flow forces acting on the car body. The noise transfer function measurements using the Laser Doppler Vibrometer (LDV) helps us to determine the resonance frequencies of the structure excited by the sound source.

This report documents the integrated approach for localising airborne and structure borne noise sources inside the vehicle with acoustic beamforming and LDV techniques to pinpoint and measure sound sources distribution inside the car. The results validate the feasibility of the integrated approach using beamforming and LDV technology, offer new insight into the distribution of interior noise sources, and provide valuable input for improved product design for quieter and comfortable cabin noise.

**Keywords**: In-cabin noise, Spherical Beamforming, Laser Doppler Vibrometry, Wind tunnel, Integrated approach

# Acknowledgements

This master's thesis topic was proposed by Volvo Car Corporation in Gothenburg and is carried out under the guidance of both Volvo Car Corporation and Applied acoustics division at Chalmers University of Technology.

First and foremost, I would like to extend a word of gratitude to Bo Karlsson and Magnus Taskinen from Volvo Car Corporation, for giving me this immense opportunity to carry out my thesis at Volvo Car Corporation. Secondly, I am greatly indebted to my supervisor Olga Roditcheva, from Volvo Car Corporation, who's constant support, guidance and technical expertise have been invaluable in the successful completion of this thesis work. I would also like to thank the wind noise team and the wind tunnel operators who helped me during the wind noise measurements in the wind tunnel.

This thesis project is the culmination of two years of study at the Division of Applied Acoustics at Chalmers University of Technology. I would like thank all my colleagues and the staff for the memorable couple of years. In particular, thank-you to my thesis supervisors, Professor Patrik Höstmad and Associate Professor Simone Sebben, who's guidance and support have helped make this thesis project a rewarding experience.

Most importantly, I would like to thank my family for their constant love and support,especially during these past two years.

Naveen Sadananda
Gothenburg, August 2016

# Contents


**List of Figures** **xi**

**List of Tables** **xiii**

**1 Introduction** **1**
1.1 Background . . . . . . . . . . . . . . . . . . . . . . . . . . . . 1
1.2 Objective . . . . . . . . . . . . . . . . . . . . . . . . . . . . 1
1.3 Thesis structure . . . . . . . . . . . . . . . . . . . . . . . . . 2

**2 Theory** **5**
2.1 In-cabin acoustics . . . . . . . . . . . . . . . . . . . . . . . . 5
2.1.1 Interior noise in automobiles . . . . . . . . . . . . . . . . . . 5
2.1.2 Wind noise . . . . . . . . . . . . . . . . . . . . . . . . . . 6
2.2 Laser Doppler Vibrometry . . . . . . . . . . . . . . . . . . . . 7
2.2.1 Doppler effect . . . . . . . . . . . . . . . . . . . . . . . . . 7
2.2.2 The Heterodyne Interferometer . . . . . . . . . . . . . . . . 9
2.3 Noise source identification techniques . . . . . . . . . . . . . . 11
2.3.1 Beamforming . . . . . . . . . . . . . . . . . . . . . . . . . 11
2.3.2 Localisation . . . . . . . . . . . . . . . . . . . . . . . . . . 11
2.3.3 Quantification . . . . . . . . . . . . . . . . . . . . . . . . . 12
2.4 Theory on flow around a structure . . . . . . . . . . . . . . . . 13

**3 Methodology** **15**
3.1 Preliminary investigations . . . . . . . . . . . . . . . . . . . . 15
3.1.1 Background noise measurement . . . . . . . . . . . . . . . . 15
3.1.2 Microphone and accelerometer measurements . . . . . . . . . 16
3.2 Noise transfer function measurements . . . . . . . . . . . . . . 17
3.3 Wind noise measurements . . . . . . . . . . . . . . . . . . . . 19
3.3.1 Overview of the tunnel . . . . . . . . . . . . . . . . . . . . 19
3.3.2 Implementation . . . . . . . . . . . . . . . . . . . . . . . . 20
3.3.3 Configurations of the car . . . . . . . . . . . . . . . . . . . 21

**4 Results and Discussion** **23**
4.1 Background noise of PVT wind tunnel . . . . . . . . . . . . . . 23
4.2 In-cabin sound pressure levels . . . . . . . . . . . . . . . . . . 23
4.3 Vibration measurements on the tailgate . . . . . . . . . . . . . 25
4.4 Mode shapes - Laser Doppler Vibrometer . . . . . . . . . . . . 25

4.5 Sound maps - wind tunnel measurements . . . . . . . . . . . . . . . . . 28
4.5.1 Interior noise without and with heavy layer . . . . . . . . . . . . 28
4.5.2 Unsteadiness and Instability of the wake . . . . . . . . . . . . . 29

**5 Conclusions and Future work 31**

**Bibliography 35**

# List of Figures


1.1 Visualisation of sound sources inside the car: red area is a significant sound source generated at the rear of the car. . . . . 2

2.1 Transmission paths of airborne and structure borne noise. . . . . 5
2.2 Propagation of sound waves - Stationary source. . . . . 7
2.3 Propagation of sound waves - Stationary receiver. . . . . 8
2.4 Working principle of Interferometer. . . . . 10
2.5 Fresnel interference pattern at time's t1 and t2. . . . . 10
2.6 A microphone array, a far-field focus direction, and a plane wave incident from the focus direction. . . . . 11
2.7 Flow pattern generated around a sphere . . . . . 13
2.8 Karman Vortex Street . . . . . 14

3.1 3-D co-ordinate system. . . . . 15
3.2 PVT Background noise measurement. . . . . 16
3.3 Microphone positions on the front and rear seats. . . . . 17
3.4 Accelerometer mounted on the tailgate. . . . . 17
3.5 Interactively defined and measured 3-D geometry, 822 measurement points. . . . . 18
3.6 Measurement setup showing the scanning heads,a vehicle ready to be measured,data acquisition and control instrumentation. . . . . 18
3.7 Position of sound source inside the car. . . . . 19
3.8 Overview of the Volvo wind tunnel with Volvo XC90. . . . . 20
3.9 Position of 3D-CAM inside the car. . . . . 20
3.10 Geometry scanning using an infrared laser unit. . . . . 21
3.11 Scanned geometry of the interior of XC90. . . . . 21

4.1 PVT Background noise level. . . . . 23
4.2 In-cabin sound pressure levels - Wind tunnel. . . . . 24
4.3 In-cabin sound pressure levels - On road. . . . . 24
4.4 Accelerometer mounted on the tailgate. . . . . 25
4.5 Mode shape at frequency 39.8 Hz. . . . . 26
4.6 Mode shape at frequency 57.5 Hz. . . . . 27
4.7 Mode shape at frequency 67.97 Hz. . . . . 27
4.8 Mode shape at frequency 83.6 Hz. . . . . 27
4.9 Mode shape at frequency 120.3 Hz. . . . . 28
4.10 Heavy layer covering the tailgate . . . . . 28

4.11 Sound map for configuration without and with HL at [0 - 26s], [90 - 100 Hz] at wind speed 130 km/h. . . . . . . . . . . . . . . . . . . . . . 29
4.12 Sound map for configuration without and with HL at [0 - 26s], [360 - 440 Hz] at wind speed 130 km/h. . . . . . . . . . . . . . . . . . . . . . 29
4.13 Sound map for configuration without and with HL at [0 - 26s], [570 - 700 Hz] at wind speed 130 km/h. . . . . . . . . . . . . . . . . . . . . . 29
4.14 Sound map for configuration at [360 - 440 Hz] at wind speed 130 km/h. 30

5.1 Microphone plot vs LDV results . . . . . . . . . . . . . . . . . . . . . . 31
5.2 Acceleromter plot vs LDV results . . . . . . . . . . . . . . . . . . . . . 32

# List of Tables


3.1 Configuration set-1. . . . . . . . . . . . . . . . . . . . . . . . . . . . . 22
3.2 Configuration set-2. . . . . . . . . . . . . . . . . . . . . . . . . . . . . 22
3.3 Configuration set-3. . . . . . . . . . . . . . . . . . . . . . . . . . . . . 22

4.1 Natural frequencies of the tailgate. . . . . . . . . . . . . . . . . . . . . . 26

# Nomenclature

$3D$ Three Dimensional

$ABN$ Air Borne Noise

$FLOE$ Front Left Outer Ear

$FT$ Fully Taped

$HL$ Heavy Layer

$HL$ Heavy Layer

$LDV$ Laser Doppler Vibrometry

$NVH$ Noise Vibration and Harshness

$RLOE$ Rear Left Outer Ear

$SBN$ Structure Borne Noise

$SUV$ Sport Utility Vehicle

$UT$ Un-taped

# 1
# Introduction

## 1.1 Background

The wind noise generated by the turbulent flow around the car is an undesirable phenomenon to the overall harmony of the vehicle. The contribution of the aerodynamic noise to the interior noise under high speed driving conditions is rising, which needs to be optimised and minimised. Hence, the minimization of wind noise in a vehicle is desirable, in which the occupants are susceptible to the background noise in the cabin, leading to discomfort and reduction in the perceived quality of the vehicle. It is hence a primary task that any windnoise concerns are analysed and resolved.

It is quite common during the development of wind noise in premium vehicles, to perform measurements in aeroacoustic wind tunnels. This allows the cabin noise to be measured by isolating other noise sources, such as the powertrain and road noise. This also allows the assessment of wind noise measured in the cabin under controlled circumstances of constant wind speed and yaw angle [2].

The noise in the vehicle cabin can be due to airborne noise transmitted directly into the cabin through gaps and leakage in the car or the structure borne noise generated due to the excitation of the certain parts of car body by the wind flow around the car. This study aims to increase the understanding of the distribution of sound sources inside the car and probable reasons for these sound sources. In order to do that, two experimental methods are used, namely the noise transfer function measurement using the Laser Doppler Vibrometer to quantify the structure borne noise sources and the second method is based on beamforming approach using the spherical acoustical array (3D-CAM) placed inside the compartment to localise the airborne sound sources.

## 1.2 Objective

The area which is the subject of interest in the proposed project is the sound source present at rear of the car. It is understood from the previous work carried out at Volvo, that a significant sound source is present at the rear of the car. The previous measurements revealed a strong sound source at the rear of the car as shown in the Figure 1.1. The measurements were performed with three-dimensional array (3D-

CAM) placed in the middle console of front seats [1]. The sound source distribution is presented for 570-700 Hz.

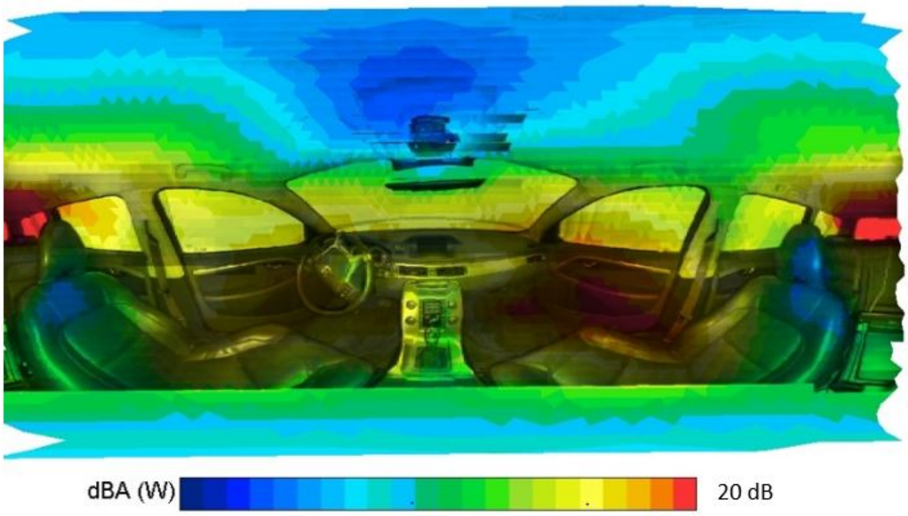


**Figure 1.1:** Visualisation of sound sources inside the car: red area is a significant sound source generated at the rear of the car.

The objective of this study is to investigate the cause of the sound source present at the rear of the car and to understand how it contributes to the interior noise levels. The resonance frequencies of the tailgate needs to be determined in order to evaluate the possibility of the turbulent flow force exciting the tailgate, which in-turn re-radiates the energy into the cabin. low frequency noise in the cabin by duse the integrated approach of noise source mapping technique alongside measuring the noise transfer functions to accurately identify, localise and quantify the noise sources on the inside of Volvo XC-90 car that will shed the light of how much noise is created by the rear wake of the car. The measurements in the present study are performed with the three-dimensional array (3D-CAM) placed in between the second and third row of the rear passenger seats to localise the sound sources at the rear of the car.

## 1.3 Thesis structure

This report consists of 6 chapters in total.

- The 1st chapter introduces the background and the objective of this project.

- The 2nd chapter describes the important theory on in-cabin nose, wind noise and the integrated approach used in the present project, namley, the Laser Doppler Vibrometry (LDV) and beamforming technique.

- The 3rd chapter explains the methodology adopted for the thesis. It deals with Laser Doppler Vibrometry measurements that was used to measure the noise transfer functions and also the spherical beamforming measurements carried out in the Volvo wind tunnel.

- The 4th chapter presents and discusses the results from various measurements performed.
- The 5th chapter presents the conclusions derived from the present work and scope of future work for the thesis.

# 2

# Theory

## 2.1 In-cabin acoustics

### 2.1.1 Interior noise in automobiles

The noise in the passenger compartment of a car is an important parameter to assess the interior sound quality in a car. A good quality car is one with good Noise, vibration and harshness (NVH) properties [3]. The noise can be classified into two categories depending on their transmission path i.e. structure borne noise (SBN) and air borne noise (ABN) . The term “borne” means to bear or to carry, therefore SBN is the vibration carried by the structure, which is then transmitted as sound energy to the inside of the car. The air borne noise is the propagation of noise directly through the air [4].

The air borne noise is transmitted directly into the cabin through gaps and leakage in the car and for the structure borne noise, the noise is usually generated by the vibrating car engine, exhaust, mounting points or the vibrating parts of the car body itself due to acoustic excitation. The vibration waves propagate through the vehicle structure of the cabin and then radiate the noise as shown in figure 2.1 [4].

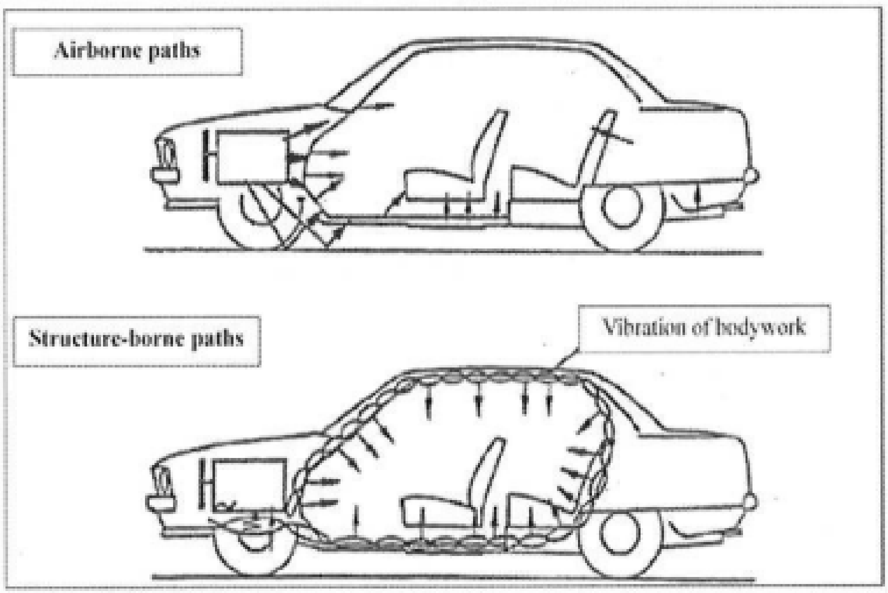


**Figure 2.1:** Transmission paths of airborne and structure borne noise.

The noise transmitted via the structure borne noise is the coupling between the structural resonance and acoustic modes inside the cabin. These modes are typically dominant at frequencies below 500 Hz. At higher frequencies, the interior noise is due to the airborne contribution caused due to tyre and wind noise [5]. Therefore, by sealing off leakages and varying the modal properties of car structure, we can reduce the airborne and structure borne noise contributions inside the car.

### 2.1.2 Wind noise

Wind noise is a predominant component of interior vehicle noise at speeds greater than 100 km/h. It is typically tested at steady vehicle speeds either on the road or in a wind tunnel. The wind noise refers to the following noise and conditions [7]:

- Aerodynamic noise made by the vehicle as it moves at high speed through a steady medium (air). This is related to the aerodynamic (or drag) coefficient of the vehicle, which is a function of the vehicle shape and its cross-sectional area.

- Aerodynamic noise due to turbulence through holes, which is correlated to how tightly sealed the vehicle is (around doors, hood, windshield etc.)

- Aerodynamic noise due to exterior varying wind conditions, such as cross-wind on a highway. This is different from the previous two, since this type of wind noise is fluctuating.

- Very low-frequency (10 to 20 Hz) beating noise occurring when either a rear window or the sunroof are partially open. This is due to the Helmholtz resonance of the vehicle cabin, which is excited by the air flow along the boundary of the window or sunroof opening.

Aerodynamically generated noise (wind noise) reaches the interior of a vehicle through various paths which includes [6]:

- Aerodynamic excitation of vibration and its re-radiation from what are known as the *greenhouse surfaces* (the roof and glass panels).

- Wind flows over and through the underbody of the vehicle with subsequent airborne transmission to the interior.

- Noise transmission through door and glass edge seals due to aspiration (leaks) or due to aerodynamic excitation of and transmission across the seals.

- Vortex shedding from vehicle appendages such as radio antennae.

## 2.2 Laser Doppler Vibrometry

Laser Doppler Vibrometry is a non-contact, 'point and shoot' technology that directly measures the vibration of a test object using the Doppler effect.

### 2.2.1 Doppler effect

The Doppler effect is the change in the observed frequency of a source due to the relative motion between the source and the receiver [8].

1. **Relative motion of the receiver**

When the source is stationary, it will emit the sound waves that propagate out from the source as shown in the Figure 2.2. As the receiver moves towards the source, it will detect the sound coming from the source but each successive sound wave will be detected earlier than it would have if the receiver were stationary.

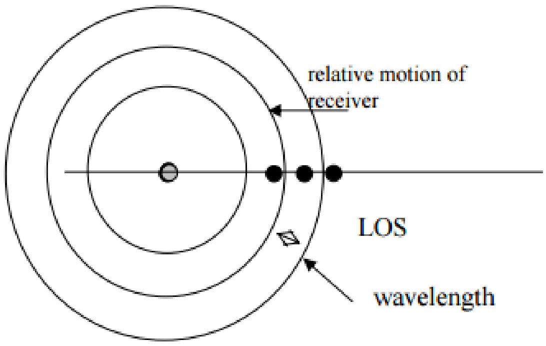


**Figure 2.2:** Propagation of sound waves - Stationary source.

Thus the frequency that each successive wave front would be detected would be changed by this relative motion, this change in the observed frequency is given by the equation 2.1,

$$\Delta f = \frac{v_r}{\lambda_o} \tag{2.1}$$

where,
$\Delta f$ = Change in the observed frequency.
$v_r$ = velocity of the receiver.
$\lambda_o$ = original wavelength of the source.

The original frequency of the sound source can be expressed as shown in below equation 2.2,

$$f_o = \frac{c}{\lambda_o} \tag{2.2}$$

where,
c = speed of sound in air.

$f_o$ = original frequency of the source.

Therefore, the observed frequency is then given by the equation 2.4,

$$f\prime = f_o + \Delta f = \frac{c}{\lambda_o} + \frac{v_r}{\lambda_o} \tag{2.3}$$

$$f\prime = f_o \left( \frac{c + v_r}{c} \right) \tag{2.4}$$

The equation 2.4 is valid only for the receiver moving towards the source, if the motion is away from the source, the relative velocity would be in the opposite direction and the equation would become,

$$f\prime = f_o \left( \frac{c - v_r}{c} \right) \tag{2.5}$$

The two equations are usually combined and expressed as,

$$f\prime = f_o \left( \frac{c \pm v_r}{c} \right) \tag{2.6}$$

**2. Relative motion of the source**

When the source is moving towards the receiver,the spacing between the wave fronts would be less as shown in the figure 2.3.

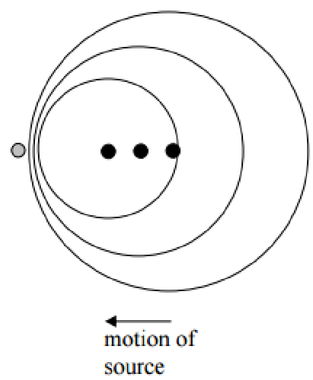


**Figure 2.3:** Propagation of sound waves - Stationary receiver.

The change in the wavelength is expressed as in equation 2.7,

$$\Delta\lambda = \frac{v_s}{f_o} \tag{2.7}$$

where,
$\Delta\lambda$ = Change in the wavelength.
$v_s$ = velocity of the source.
$f_o$ = original frequency of the source.

Therefore, the observed frequency is then given by the equation 2.9,

$$f\prime = f_o + \Delta f = \frac{c}{\lambda_o} + \frac{v_s}{\lambda_o} \tag{2.8}$$

$$f\prime = f_o \left( \frac{c}{c - v_s} \right) \tag{2.9}$$

The equation 2.9 is valid only for the source moving towards the receiver, if the motion is away from the receiver, the relative velocity would be in the opposite direction and the equation would become,

$$f\prime = f_o \left( \frac{c}{c + v_s} \right) \tag{2.10}$$

The two equations are usually combined and expressed as,

$$f\prime = f_o \left( \frac{c}{c \mp v_s} \right) \tag{2.11}$$

Therefore, the Doppler equation can be given as in equation 2.12,

$$f\prime = f_o \left( \frac{c \pm v_r}{c \mp v_s} \right) \tag{2.12}$$

When a wave is reflected by a moving object and detected by a measurement system (as is the case with the LDV), the measured frequency shift '$F_d'$ of the wave can be defined as in equation 2.13,

$$f_d = 2\frac{v}{\lambda} \tag{2.13}$$

where,
v = object's velocity.
$\lambda$ = wavelength of the emitted wave.

To be able to determine the velocity of an object, the (Doppler) frequency shift has to be measured at a known wavelength. This is done in the LDV by using a laser interferometer [8].

### 2.2.2 The Heterodyne Interferometer

Figure 2.4 shows the working principle of laser vibrometer's head. A laser beam is directed normal onto a vibrating surface. If the surface moves towards the laser source, the waves will be compressed, while when moving away it will stretch the waves.

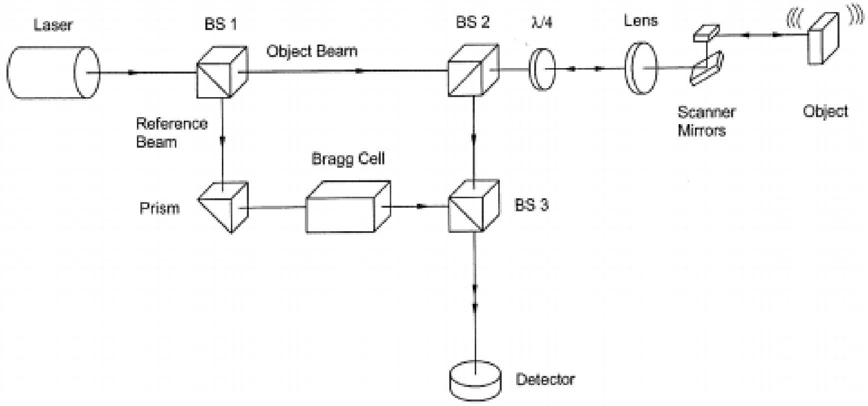


**Figure 2.4:** Working principle of Interferometer.

The beam of a helium neon laser is split by a beam splitter (BS 1) into a reference beam and a measurement beam. After passing through a second beam splitter (BS 2), the measurement beam is focused on to the object under investigation, which reflects it. This reflected beam is now directed downwards by BS 2, is then merged with the reference beam by the third beam splitter (BS3) and is then directed on to the detector. Due to the time difference, the two beams will have frequency and phase shifts which result in an interference pattern, looking like Fresnel zones as shown in figure 2.5. The pattern which is time varying gives the information about the velocity of the surface vibration. It is detected by a photo detector and it transformed into a voltage signal.

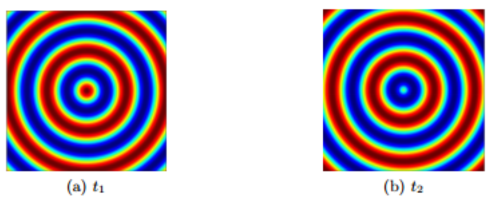


**Figure 2.5:** Fresnel interference pattern at time's t1 and t2.

The Bragg cell performs a frequency shift for the reference beam. The interference between the original reference light and reflected beam will be measured as a frequency difference. However, the detector knows only the magnitude but not the sign of the difference. By shifting the frequency of the reference beam, already when the surface is in rest the sensor would measure a modulation frequency (the shift). If the surface moves now towards the laser, this frequency will be decreased and if it moves away, it will be increased. Now, the absolute value of the frequency difference gives the desired direction information [9].

## 2.3 Noise source identification techniques

The noise source identification techniques (NSI) are used to localise the sound sources and optimise the noise emission from a wide range of products such as automobiles, consumer products, aeroplanes and many more. The goal of NSI is to identify the most important sound sources on an object in terms of position, frequency content and sound power radiation [10].

### 2.3.1 Beamforming

Beamforming is an array based technique for sound source localisation for low to mid frequency range. Beamforming has become a popular technique for noise source identification for exterior vehicle noise and for localising interior vehicle noise in wind tunnels.

Beamforming is suited for far-field measurements where sound waves act as planar waves and the beamforming array can be a planar array or a spherical array depending on the application. The classical beamforming involves placing a planar array of microphones in a plane externally to the vehicle. This allows the identification of sound sources within the plane at a defined distance from the array. However, for in-cabin measurements, noise sources may be present on all sides of the antenna. The reflections within the cabin can lead to ghost images. Hence a planar array cannot be used in the cabin, since such an array is unable to separate sources behind and in front of the antenna. Therefore, a three dimensional array (3D CAM) is used for in-cabin noise measurements.[11]

### 2.3.2 Localisation

The principle used for localisation is the Delay-and-Sum beamformer. Let us consider a planar array of 'M' microphones at locations $r_m$ (m=1,2,...M) in the x-y plane as shown in the figure 2.6. In Delay-and-Sum beamforming, the measured pressure signals are individually delayed and summed.

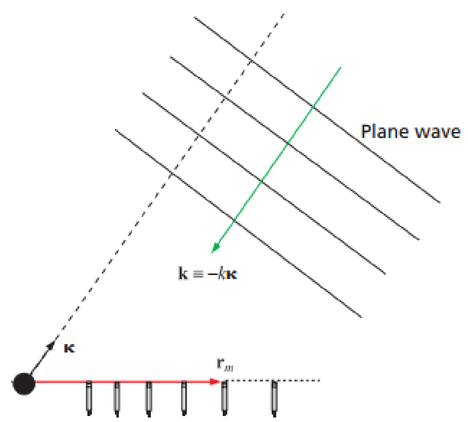


**Figure 2.6:** A microphone array, a far-field focus direction, and a plane wave incident from the focus direction.

Consider the equation 2.14 which describes the Delay-and-Sum beamforming principle when applied to the array considered in figure 2.6.

$$b(k,t) = \sum_{m=1}^{M} w_m p_m(t - \Delta_m(k)) \tag{2.14}$$

where,
$w_m$ = weighting coefficients applied to individual microphone signals.
$\Delta_m$ = time delays applied to individual microphone signals.
k = unit vector
$p_m$ = measured pressure signals

The Delay-and-Sum beamformer simply delays each microphone output with a delay of $\Delta_m$ so that the signal components from the desired source are synchronised across all sensors. This objective is met by adjusting the time delays in such a way that signals associated with a plane wave, incident from the direction 'k', will be aligned in time before they are summed. These signals are then weighted and summed together reinforcing signals coming from the desired direction to produce the beamformer output. The signals arriving from other far-field directions will not be aligned before the summation, and therefore they will not add up coherently, thus obtaining a directional sensitivity [11].

### 2.3.3 Quantification

Equivalent source method (ESM) is an advanced sound source localisation processing which is quantitative. It is an inverse method that provides an estimation of the source volume velocity and thus characterises the sound power level of a source. Secondly, ESM sound source localisation processing has a better resolution in low frequency and a better dynamic range at high frequencies than beamforming processing.

The principle of this method considers that the real sources can be replaced with a superposition of equivalent sources placed at the calculation points. The equivalent volume velocities *[q]* at these calculation points are linked with measured sound pressures $[p_m]$ by a transfer function *[H]*. The inverse problems tend to find a solution to a system of equation modeled by equation 2.15.

$$Hq = p \tag{2.15}$$

In case of noise source identification with a sphere, the microphone pressures around the sphere form the $p$ vector. The sound monopole sources are referred to $q$ components: the inverse method has no restriction on the source distribution geometry. Their distribution is issued from the discretisation of the cavity space with the security to correctly separate noise source direction with the presence of the solid sphere in its centre. The *[H]* matrix of the solid sphere modifies the propagation of acoustic waves around its circumference scattering the incident field. The expression of one element from the *[H]* matrix includes the spherical harmonics expansion induced by the sphere diffraction is given by equation 2.16.

$$p(r, a, \omega, \theta, t) = \frac{i\rho c Q}{4\pi a^2} \Psi e^{-i\omega t} \tag{2.16}$$

The number of sources is superior to the measurement points in order to get a fine spatial discretisation of the cavity. As a consequence, the number of rows for H is superior to the number of columns leading to several solutions. The difficulty is to find the best solution. The method which is usually used firstly decomposes the H matrix into singular value of the form as given in equation 2.17 [12].

$$SVD(H^*_{[m,s]}) = V_{[s,m]} S_{[m,m]} U^*_{[m,m]} \tag{2.17}$$

The system can now be expressed as in equation 2.18,

$$U_{[m,m]} S_{[m,m]} V^*_{[s,m]} q = p \tag{2.18}$$

## 2.4 Theory on flow around a structure

The flow past the rear of the car smoothly divides and reunites at lower wind speeds. As the wind speed increases, the flow separates in the downstream and the wake is formed by two symmetric eddies. The eddies remain steady and symmetrical but grow in size. At very high wind speeds, the wake starts shedding vortices into the stream. A hopf bifurcation breaks the symmetry between the two eddies and with a slight bifurcation the vortex detaches itself from the body. In its place a new vortex is formed. At very high value of Reynold's number, eddies shed continuously from each side of the body forming rows of vortices in its wake. As an illustration, the flow past a sphere is shown in Figure 2.7.

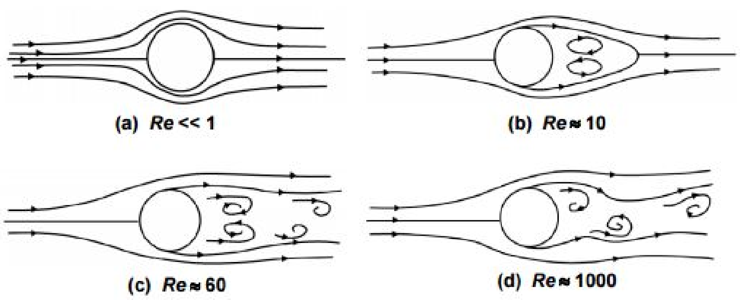


**Figure 2.7:** Flow pattern generated around a sphere

The vortices are shed into the downstream flow from alternate sides of the body with alternate senses of rotation, giving the apperance of alternately opposite signed vortices. The similarity of the wake with the footprints in a street, the staggered row of vortices behind the body is called the Karman Vortex street. While an eddy on one side is shed, that on the other side forms, resulting in a unsteady flow near the tailgate. As vortices of opposite circulations are shed off alternately from the two sides which forms the pattern as shown in Figure 2.8, the circulation around the tailgate changes sign, resulting in a lateral force. If the frequency of vortex shedding is close to the natural frequency of some mode of vibration of the tailgate structure, then an appreciable lateral vibration culminates. This may cause large fluctuating pressure forces leading to structural vibrations, acoustic noise or resonance. When the frequency of vortex shedding matches the resonance frequency of the structure, the structure will begin to resonate and the structure's movement can become self-sustaining [13].

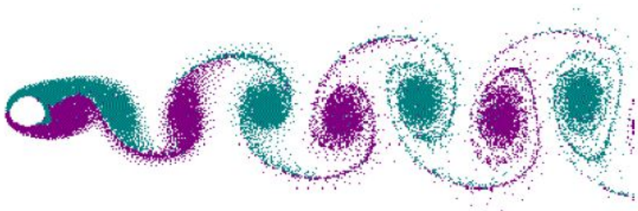

**Figure 2.8:** Karman Vortex Street

# 3
# Methodology

## 3.1 Preliminary investigations

The preliminary investigations include the measurement of background noise in the wind tunnel to assess the influence of the background noise on the actual measurements. The preliminary check also involves the measurements with microphone and accelerometer mounted on the rear seat and on the tailgate respectively, in order to quantify the sound pressure levels, vibration levels and also to investigate any significant peaks at any particular frequency.

The preliminary investigations are performed in the wind tunnel at a wind speed of 130 km/h. The figure 3.1 represents the co-ordinate system followed for all the measurements in this project. The Z-axis is along the length of the car, Y-axis represents upward direction and X-axis represents sideways.

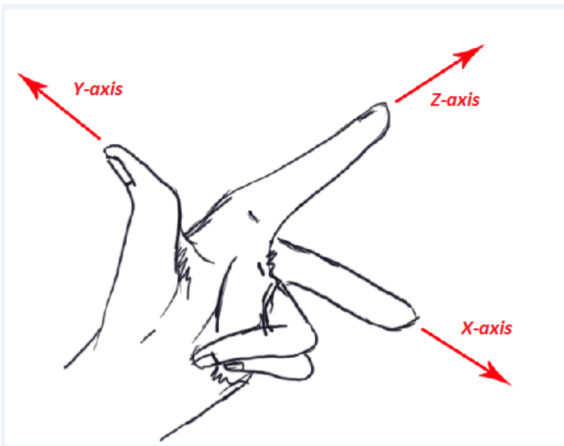


**Figure 3.1:** 3-D co-ordinate system.

### 3.1.1 Background noise measurement

The background noise measurements were performed in order to determine the contribution of the wind tunnel to the actual measurements. The background noise in the PVT wind tunnel was measured at a wind velocity of 90, 120 and 130 km/h. This is the velocity which is used for requirement settings at Volvo Cars and is the main velocity of interest for the measurements in our project. The measurements were done without the car at several positions in the wind tunnel: close to the inlet, in the middle of the test section, close to the walls, close to the outlet as shown in figure 3.2 and it also shows one such position where the background noise was measured with the help of two microphones with nose cone and wind screen on each of the microphone.

The background sound pressure levels were recorded at different positions in the wind tunnel. The microphone was mounted using a stand with a magnetic foot which locks the stand and keeps the microphone in place under wind conditions. The nose cone microphones were used for the measurements, to minimise the aerodynamically induced noise caused when the microphone is exposed to high wind velocities. The microphone was positioned parallel to the wind flow.

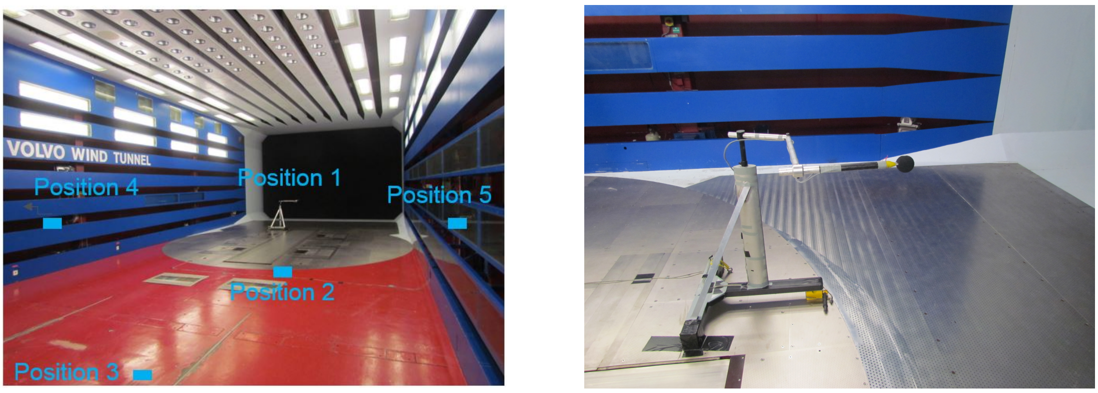


**Figure 3.2:** PVT Background noise measurement.

### 3.1.2 Microphone and accelerometer measurements

The microphones were mounted at the occupants ear level on both front and rear seats as shown in figure 3.3, while the accelerometer was mounted on the inside of tailgate as shown in figure 3.4.

**Figure 3.3:** Microphone positions on the front and rear seats.

**Figure 3.4:** Accelerometer mounted on the tailgate.

## 3.2 Noise transfer function measurements

The structural vibration measurements can be conveniently classified into two types,

- Discreet point measurements using accelerometers or any equivalent transducers.
- Spatial field measurements using the interferometry technique.

In the present project, the Laser Doppler Vibrometer (LDV) is used to measure the structural vibrations of the tailgate of the car under investigation i.e. Volvo XC90 car.

Firstly, the surface of the tailgate is prepared by spraying a white reflective paint, so that the surface is retro-reflective i.e. there are reflections in multiple reflection angles and ensure the signal-to-noise ratio is good. The scan points of the geometry are then defined interactively. During interactive scan point definition, the 3-D coordinates are determined by the integrated geometry scanner. The outcome of the geometry measurement with scan points is as shown in figure 3.5.

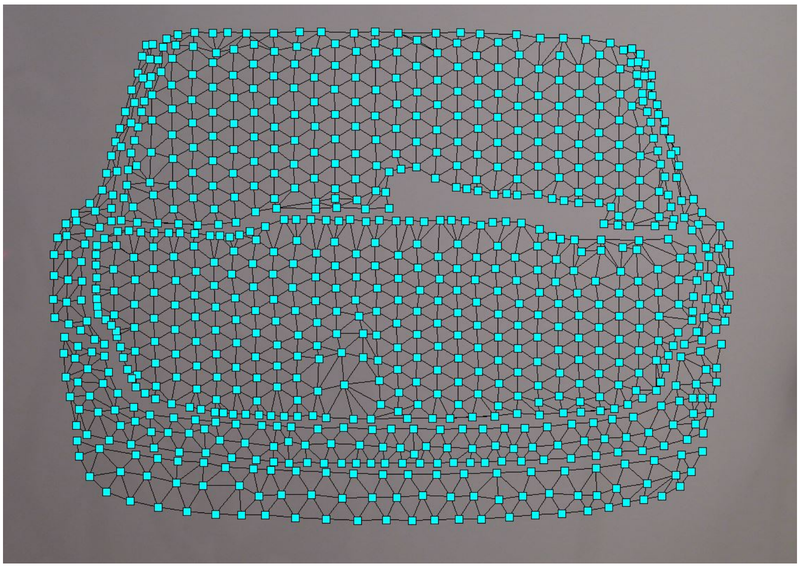

**Figure 3.5:** Interactively defined and measured 3-D geometry, 822 measurement points.

The position of the laser heads are defined, from which the measurement is carried out. Once all the measurement points are defined, a calculation is carried out to verify which measurement points can be reached ideally from which position. The software examines the angle of incidence of the laser beams on the surface as well as possible shadowing. Figure 3.6 shows an installation with three laser heads and the tailgate of the car under investigation.

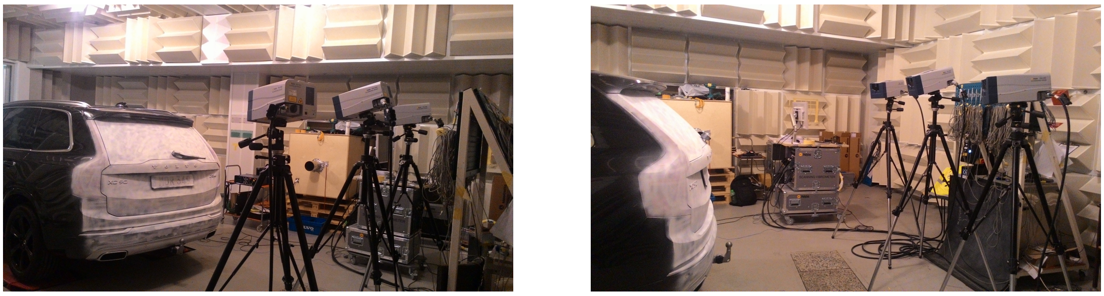

**Figure 3.6:** Measurement setup showing the scanning heads,a vehicle ready to be measured,data acquisition and control instrumentation.

For the test, the vehicle is excited by a volume acceleration sound source placed inside the car as shown in the figure 3.7. The input applied via the sound source is measured using an accelerometer and the volume acceleration is considered which indicates the source strength. The accelerometer used to measure the input is also used as a reference signal for all measurements. The output generator controls the sound source and a periodic chirp signal is used for excitation.

**Figure 3.7:** Position of sound source inside the car.

The measurement process is triggered with a trigger signal which triggers the next measurement respectively as soon as a measurement position is reached. This measurement includes approx. 822 scan points. For this test, the total measurement time was approx. 4.5 hours.

## 3.3 Wind noise measurements

### 3.3.1 Overview of the tunnel

The wind noise measurements were carried out in the PVT wind tunnel at Volvo Car Corporation. The tunnel is designed aerodynamically and not aeroacoustically. Hence the tunnel has good flow properties, but the size and shape of the test section and the fan location influence the the results of the wind noise measurements.

The PVT wind tunnel is as shown in the figure 3.8. The left hand side of the tunnel has a steel slotted wall and behind this, is the wall of the wind tunnel which is acoustically treated. On the right hand side of the test section, the slotted wall has the same construction but with transparent glass so that the control room has a clear view of the tunnel. Behind the slotted wall on the right hand side, there are several glass panels, which is provided to facilitate the test engineers to have a clear view of the test section during the experiment. The asymmetry of the tunnel and the rigid slotted walls are the strong factors influencing the quality of the wind noise measurements.

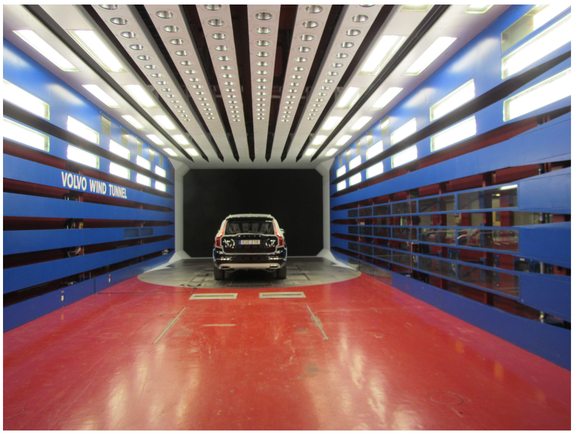


**Figure 3.8:** Overview of the Volvo wind tunnel with Volvo XC90.

### 3.3.2 Implementation

The vehicle under investigation was a Volvo XC90 and the car was tested in fully taped condition. The car was fixed to the floor and a non-rotating wheel condition was used during the wind noise measurements. The interior measurements were carried out using the LMS 3D-CAM spherical array with 36 microphones for localisation and visualisation of sound sources inside the car. The spherical array was positioned in the rear of the car with all the rear seats down as shown in the figure 3.9.

**Figure 3.9:** Position of 3D-CAM inside the car.

The geometry of the car was scanned using an infrared laser as shown in figure 3.10 and a grid of 3600 triangular elements was used to get a finer resolution of the geometry as shown in figure 3.11.

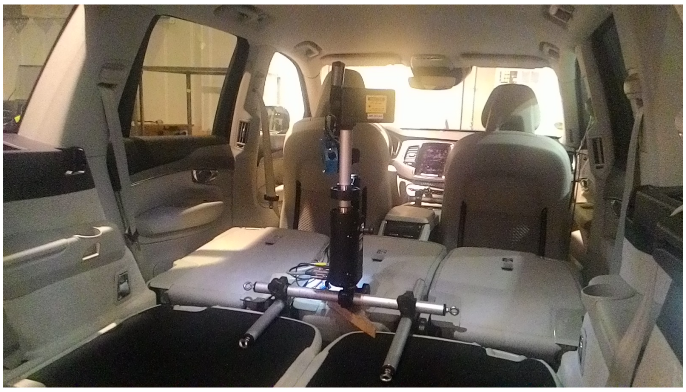

**Figure 3.10:** Geometry scanning using an infrared laser unit.

**Figure 3.11:** Scanned geometry of the interior of XC90.

### 3.3.3 Configurations of the car

The wind noise measurements were carried out for various configurations on XC90 as shown in the following tables 3.1, 3.2 and 3.3 to investigate and troubleshoot the interior noise of the XC90.

**Table 3.1:** Configuration set-1.

| *Configuration* | *Velocity(km/h)* | *Yaw angle* | *Heavy layer* |
|---|---|---|---|
| FT-Shutter open | 90 | 0 | NO |
| FT-Shutter open | 90 | 10 | NO |
| FT-Shutter open | 90 | -10 | NO |
| FT-Shutter open | 110 | 0 | NO |
| FT-Shutter open | 110 | 10 | NO |
| FT-Shutter open | 110 | -10 | NO |
| FT-Shutter open | 130 | 0 | NO |
| FT-Shutter open | 130 | 10 | NO |
| FT-Shutter open | 130 | -10 | NO |

**Table 3.2:** Configuration set-2.

| *Configuration* | *Velocity(km/h)* | *Yaw angle* | *Heavy layer* |
|---|---|---|---|
| FT-Shutter open | 90 | 0 | YES |
| FT-Shutter open | 90 | 10 | YES |
| FT-Shutter open | 90 | -10 | YES |
| FT-Shutter open | 110 | 0 | YES |
| FT-Shutter open | 110 | 10 | YES |
| FT-Shutter open | 110 | -10 | YES |
| FT-Shutter open | 130 | 0 | YES |
| FT-Shutter open | 130 | 10 | YES |
| FT-Shutter open | 130 | -10 | YES |

**Table 3.3:** Configuration set-3.

| *Configuration* | *Velocity(km/h)* | *Yaw angle* | *Heavy layer* |
|---|---|---|---|
| FT - Shutter closed - Inside cavity closed | 130 | 0 | NO |
| FT - Shutter closed - Inside cavity closed | 130 | 0 | YES |

# 4

# Results and Discussion

## 4.1 Background noise of PVT wind tunnel

The background noise levels for different wind speeds with microphone at position 2 is as shown in figure 4.1. The results from position 2 is chosen, since it was in the middle of the wind tunnel and approximately a meter away from any surfaces to avoid reflections. The overall background noise levels increases approximately 4 dB with increase in wind speed. The background noise levels have significant peaks at frequencies 41 Hz, 83 Hz and 151 Hz for all wind speeds. However, at 130 km/h wind speed there exists another peak at 25 Hz which is not present for lower wind speeds. The peak at 41 Hz and 83 Hz does not change in frequency irrespective of the wind speed unlike the peak at 151 Hz which shifts in frequency as wind speed increases.

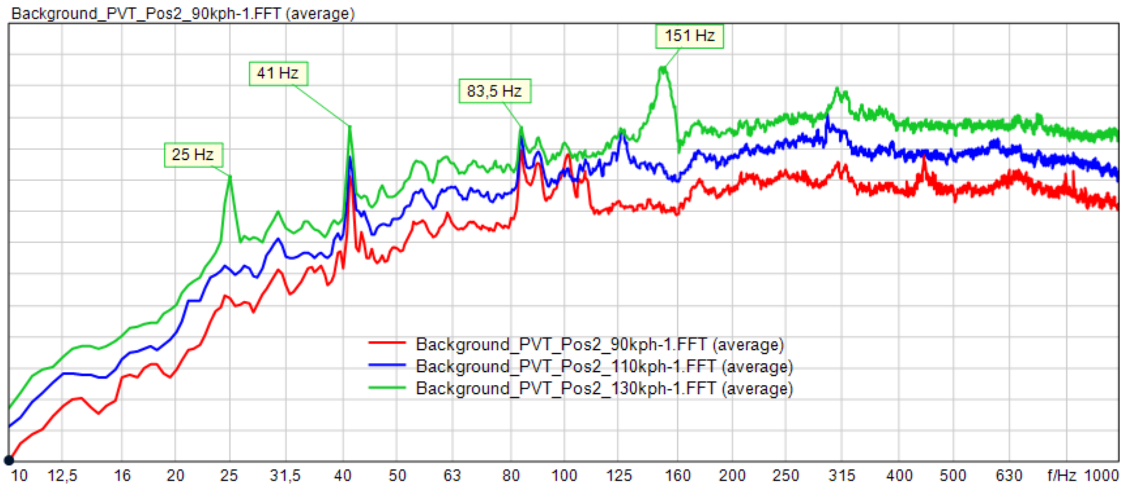


**Figure 4.1:** PVT Background noise level.

## 4.2 In-cabin sound pressure levels

The sound pressure levels inside the car measured in the wind tunnel at 130 km/h wind speed is as shown in figure 4.2. The overall sound pressure levels are approximately the same for both FLOE and RLOE positions respectively. We observe significant peaks at certain frequencies as shown in the plot, which needs to be further investigated.

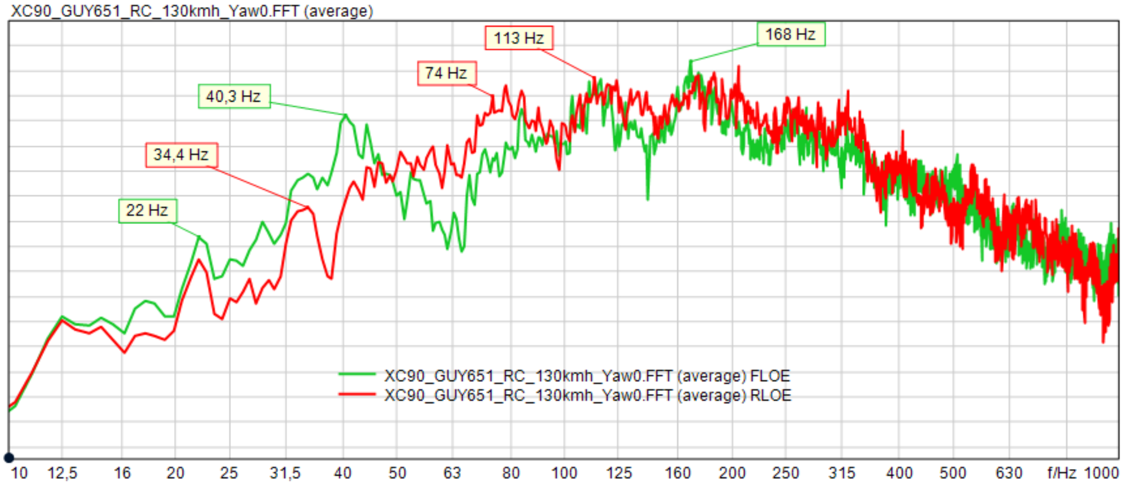


**Figure 4.2:** In-cabin sound pressure levels - Wind tunnel.

With the same microphone positions inside the car, the interior sound pressure levels were measured with the car operating on road at 130 km/h. The sound pressure level plot is as shown in the figure 4.3 with significant peaks highlighted using cursors.

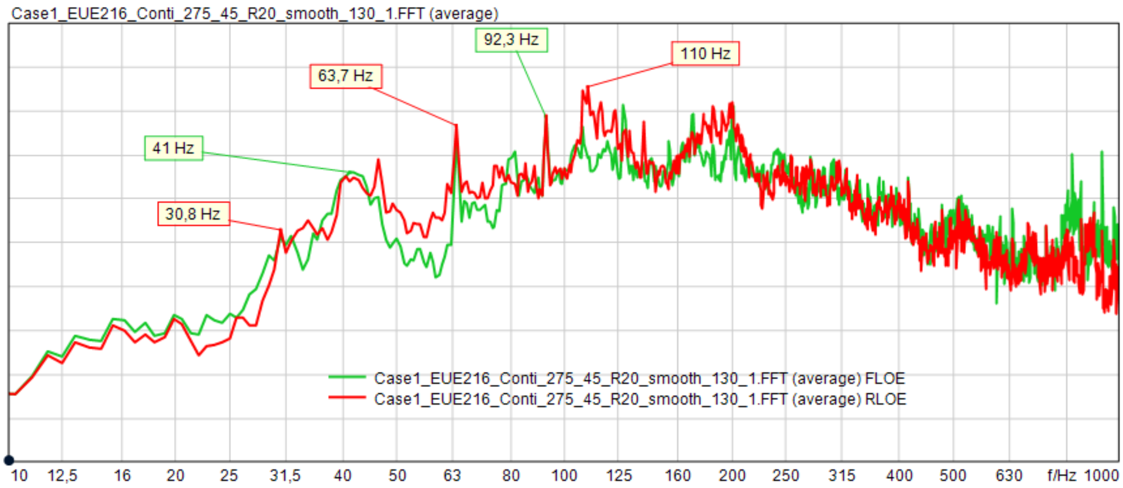


**Figure 4.3:** In-cabin sound pressure levels - On road.

The plots for the in-cabin sound pressure levels measured in the wind tunnel and on road exhibit similar characteristics with peaks approximately at the same frequencies 30 Hz, 40 Hz, 65 Hz and 110 Hz in both conditions. Hence, it can be considered as the characteristic of the car which results in these significant peaks and not due to the background noise levels. In order to further investigate these low frequency peaks in the microphone measurements, vibration measurements and LDV measurements were carried out to evaluate the structural characteristics of the tailgate structure.

## 4.3 Vibration measurements on the tailgate

In order to further investigate the peaks that appear in the microphone measurements, vibration measurements with an accelerometer was performed as well. The accelerometer was mounted on the inner surface of the tailgate. The results of the measurements are illustrated in figure 4.4. In this plot, the peaks at approximately the same frequency can be observed in all the three directions, but it is more significant in the Z-direction which is along the length of the car. This possibly indicates that the tailgate area is excited by the turbulent flow of the wind around the wake of the car around 40 Hz which corresponds to the first resonance frequency of the tailgate.

Further, to understand these low frequency peaks from the accelerometer measurements, the noise transfer functions were measured using the Laser Doppler Vibrometer. The LDV measurements were performed to ascertain if these peaks were caused due to the resonant behaviour of the tailgate excited by the turbulent flow of the wind. The results of the same are presented in the subsequent section.

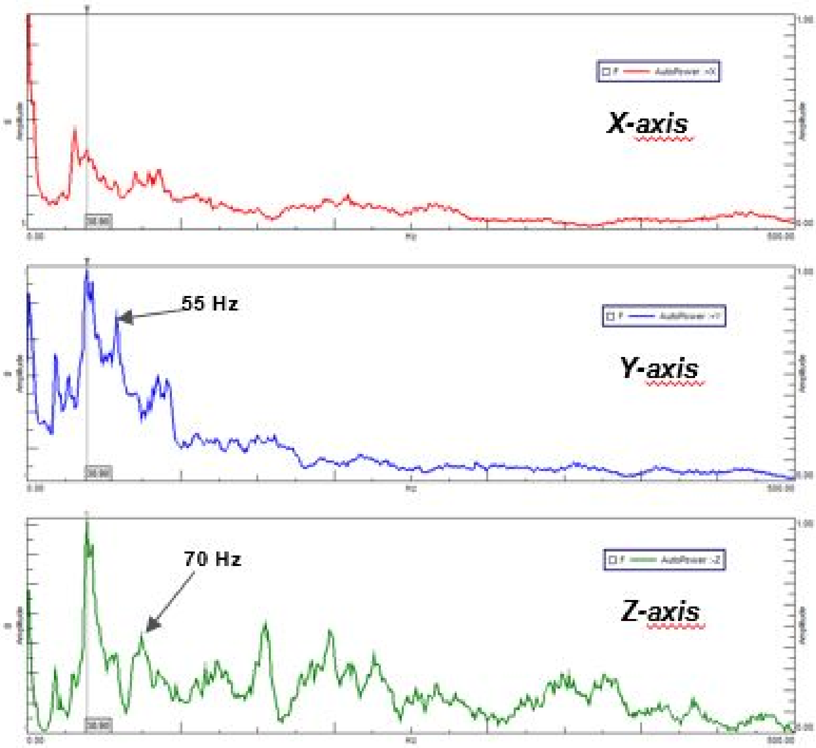


**Figure 4.4:** Accelerometer mounted on the tailgate.

## 4.4 Mode shapes - Laser Doppler Vibrometer

The LDV measurements highlighted new, previously hidden noise sources. One of them is aerodynamically induced component vibration, created by the interaction of non-stationary flows and the vehicle's structure. In the present case, the tailgate is induced to vibrate by the flows around them and transmit the resultant energy into the vehicle cabin in the form of vibration or sound.

The cause of structural vibration in response to aerodynamic inducement is turbulence. In very simplified terms, the turbulence can be regarded as a series of so-called “Eddies” which float past the surface. These Eddies create high variable pressures on the surface, which correlate with each other and move over the surface of the component at a certain velocity – the so-called convection velocity – in the direction of the wind. [14]

Table 4.1 lists the natural frequencies for the tailgate structure and the subsequent figures 4.5 to 4.9 shows the mode shapes (structural deformation) at each of the natural frequencies of the tailgate. From the mode shapes it can be observed that, the first mode at 39.8 Hz is a pumping mode and the second mode at 57.5 Hz is a bending mode which shows the structural deformation of the tailgate. The third, fourth and the fifth modes are higher orders of pumping mode.

**Table 4.1:** Natural frequencies of the tailgate.

| *Mode number* | *Frequency (Hz)* |
|---|---|
| Mode 1 | 39.8 |
| Mode 2 | 57.5 |
| Mode 3 | 67.9 |
| Mode 4 | 83.6 |
| Mode 5 | 120.3 |

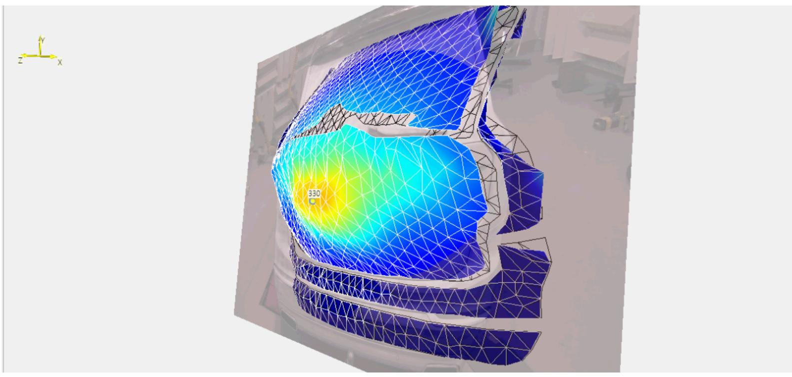

**Figure 4.5:** Mode shape at frequency 39.8 Hz.

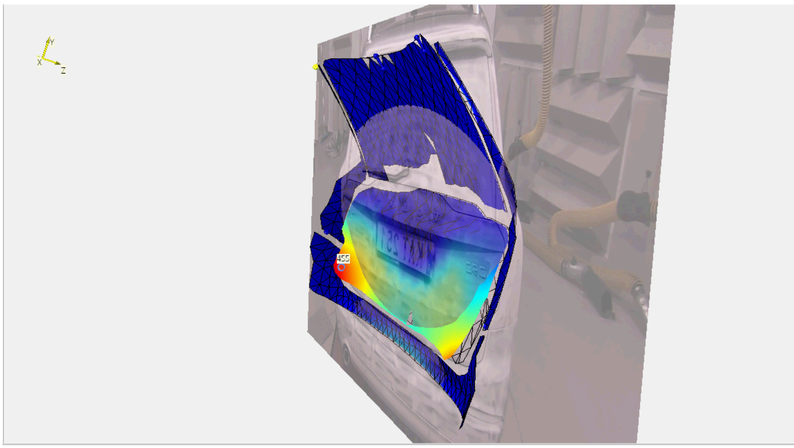

**Figure 4.6:** Mode shape at frequency 57.5 Hz.

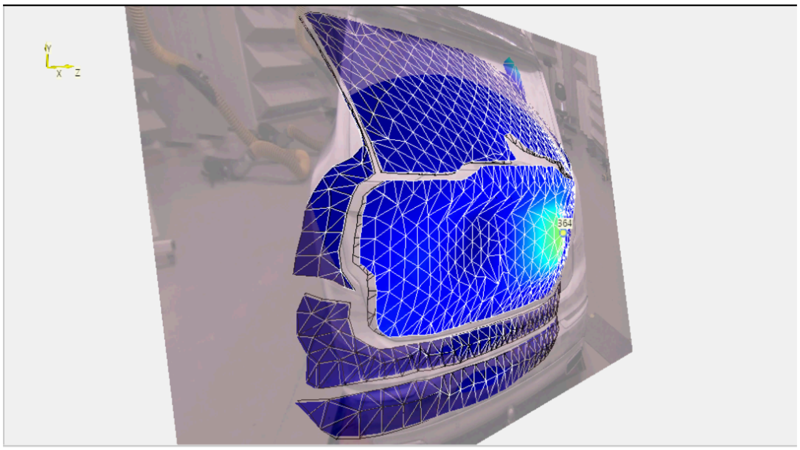

**Figure 4.7:** Mode shape at frequency 67.97 Hz.

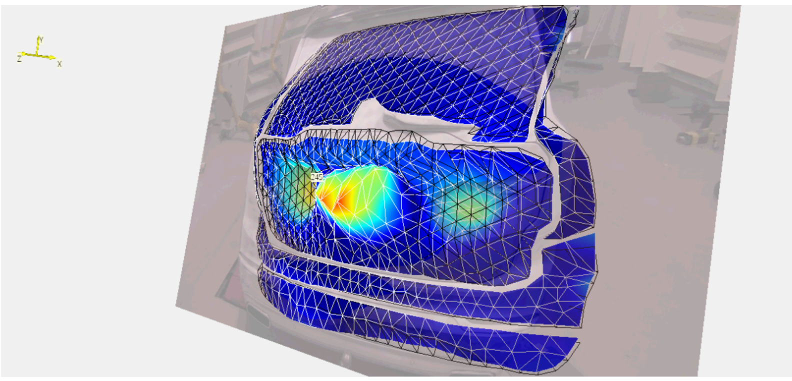

**Figure 4.8:** Mode shape at frequency 83.6 Hz.

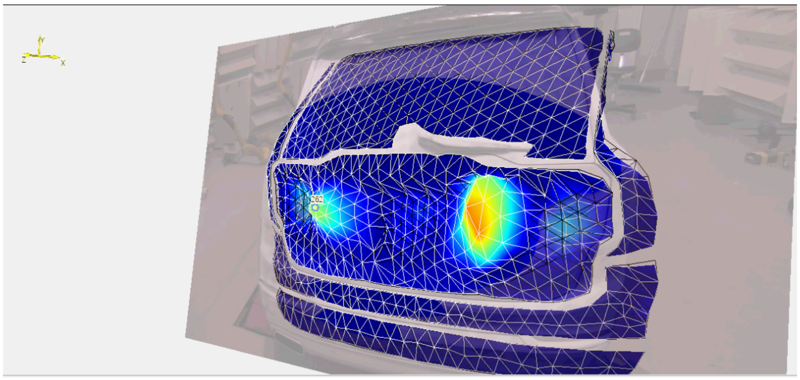

**Figure 4.9:** Mode shape at frequency 120.3 Hz.

## 4.5 Sound maps - wind tunnel measurements

### 4.5.1 Interior noise without and with heavy layer

The figures 4.11 to 4.13 show the comparison of the interior noise with and without heavy layer. The tailgate of the car is less damped and less stiff which makes it to vibrate due to turbulent flow force excitation around the tailgate. Hence, it was decided to investigate the interior noise by increasing the damping of the tailgate using a heavy layer. A heavy layer consists of a layer of stiff rubber and a thick layer of foam that glued to the rubber layer. The heavy layer was positioned as shown in the Figure 4.10 covering the metal part of the tailgate. The heavy layer adds some mass and damping to the tailgate area which in turn reduces the sound pressure levels inside the car. It is evident from the sound maps that, there is a decrease in the interior noise by the use of heavy layer.

**(a)** **(b)**

**Figure 4.10:** Heavy layer covering the tailgate

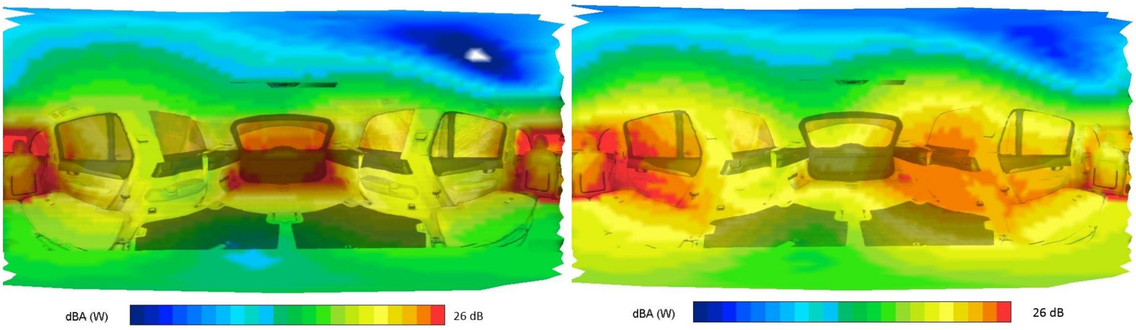


(a) Without heavy layer. (b) With heavy layer.

**Figure 4.11:** Sound map for configuration without and with HL at [0 - 26s], [90 - 100 Hz] at wind speed 130 km/h.

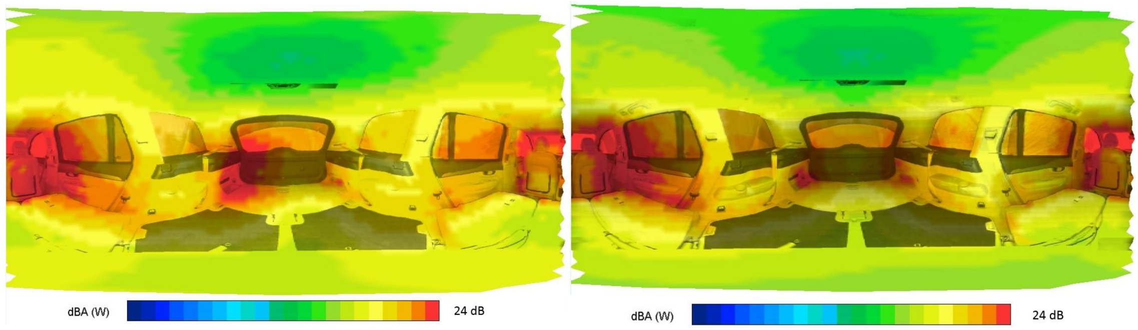


(a) Without heavy layer. (b) With heavy layer.

**Figure 4.12:** Sound map for configuration without and with HL at [0 - 26s], [360 - 440 Hz] at wind speed 130 km/h.

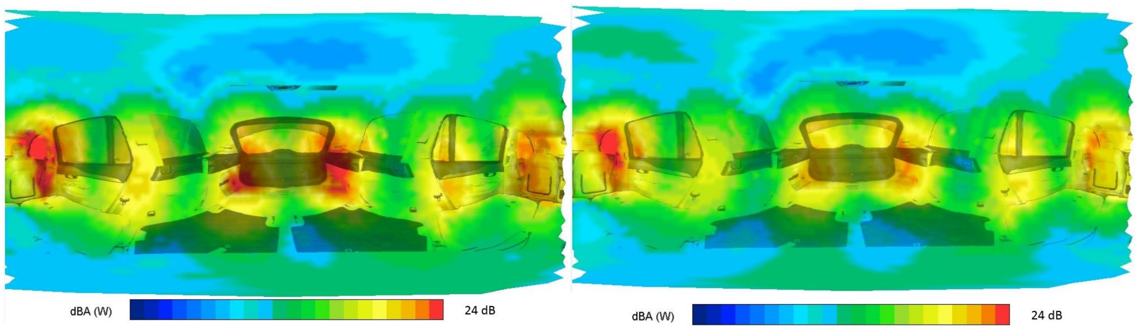


(a) Without heavy layer. (b) With heavy layer.

**Figure 4.13:** Sound map for configuration without and with HL at [0 - 26s], [570 - 700 Hz] at wind speed 130 km/h.

### 4.5.2 Unsteadiness and Instability of the wake

The data from 3D CAM was acquired for 120 seconds at 130 km/h wind speed. The acquired data is post processed at every 3 seconds to extract sound maps. The unsteadiness of the wake can be observed from the sound maps obtained from the wind tunnel measurements. The wake tends to behave transiently i.e. the sound source changes it position with time as shown in the figure 4.14. The hot spot patterns repeats after a certain interval, causing low frequency variable pressure on the surface of the the tailgate as explained in section 2.4.

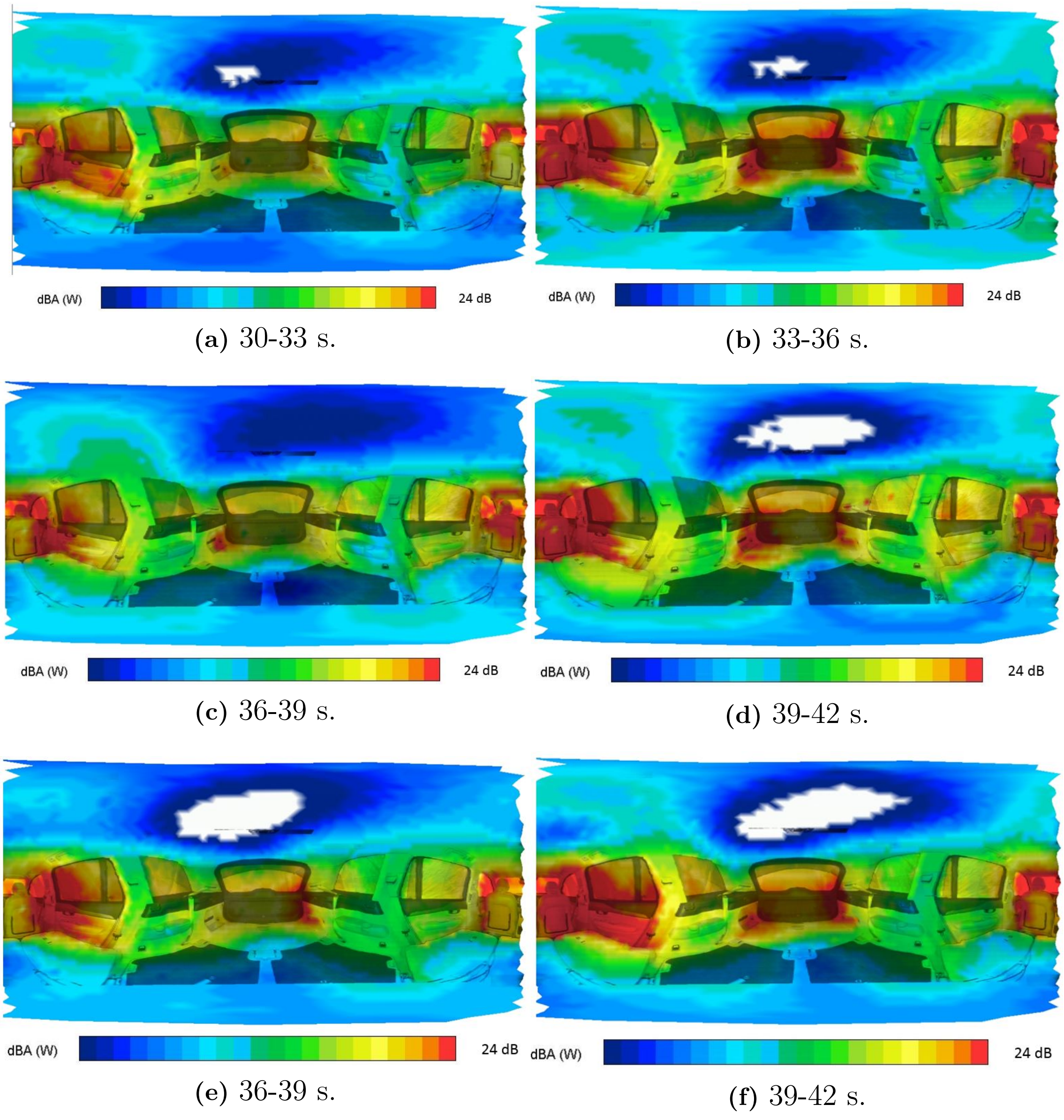


**(a)** 30-33 s. **(b)** 33-36 s. **(c)** 36-39 s. **(d)** 39-42 s. **(e)** 36-39 s. **(f)** 39-42 s.

**Figure 4.14:** Sound map for configuration at [360 - 440 Hz] at wind speed 130 km/h.

# 5
# Conclusions and Future work

The peaks observed in the background noise plots could possibly be due to the wind tunnel modes. Although it seems like the peaks in the background noise plot does not contribute to the interior noise, it is necessary to investigate the reason and understand the peaks in the background plots.

From the interior noise plots from the wind tunnel and on road conditions, the characteristic of the curve is similar in both conditions. Thus, it can be inferred that, the peaks observed in these peaks are due to the inherent properties of the structure. The laser doppler vibrometer results reveals the resonant frequencies of the tailgate and the mode shapes for the resonant frequencies. It can be observed from the mode shapes that the structure resonates with higher amplitude along the Z-axis, which indicates that the structure is less stiff along the Z-axis. The low frequency peaks observed in the microphone and accelerometer measurements might be caused due to the resonant behaviour of the tailgate structure or due to transmission of energy to other parts causing it to vibrate, as shown in the figure 5.1 and 5.2, which shows the resonant peaks matching closing with the low frequency peaks.

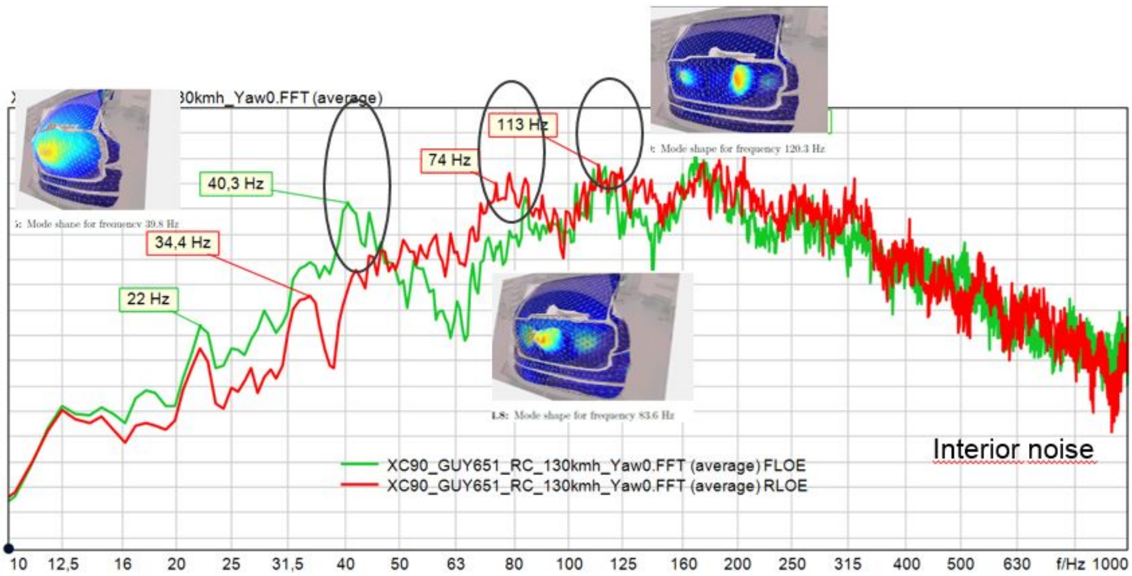


**Figure 5.1:** Microphone plot vs LDV results

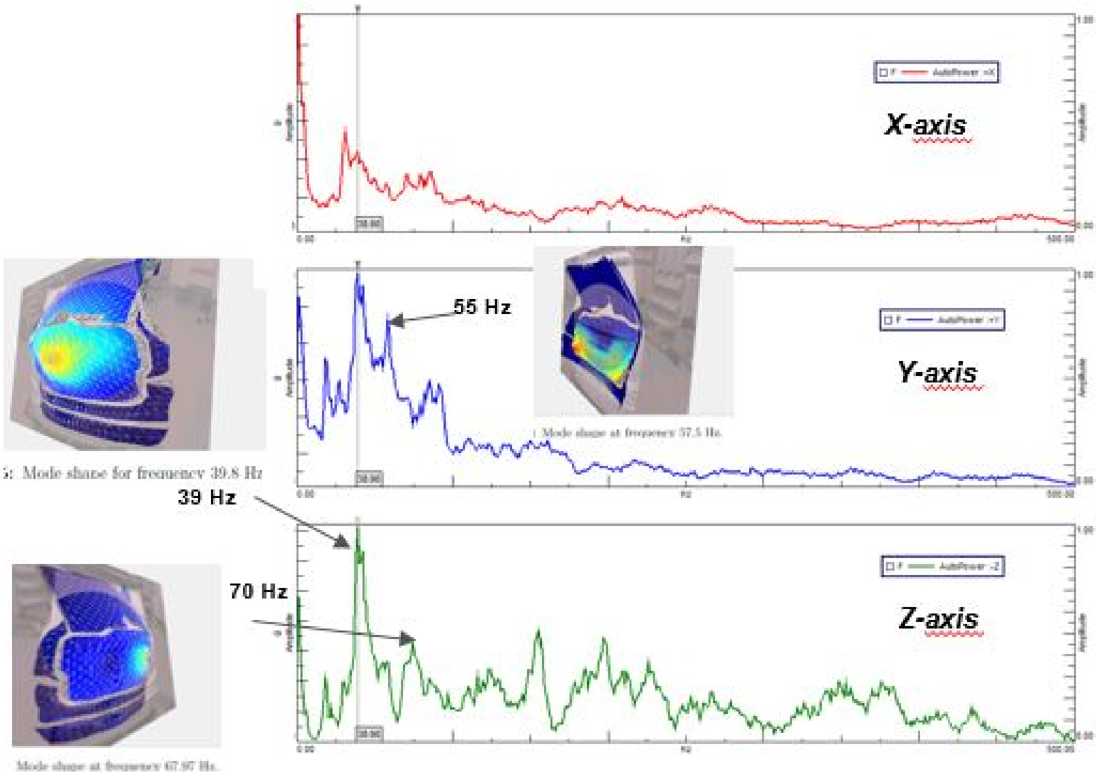


**Figure 5.2:** Acceleromter plot vs LDV results

The low-frequency variable pressures created by flows over the vehicle body cause body parts to vibrate over a broad band. This either leads directly to sound emission into the vehicle cabin, or may transmit energy to other components by other paths, thereby inducing them to vibrate in turn. From the 3D beamforming sound maps, the sound sources are localised on the rear of the car. These sound sources are possibly due to the energy being radiated into the cabin due to the vibration of the tailgate.

The problems arising as a result of this can at present only be identified at a very late stage in the development process, when eliminating them is likely to incur high cost. The consequence is often that stiffeners or mass elements are retrofitted, greatly impairing the success of the lightweight construction concept. Additionally, it is often difficult to identify the cause of low-frequency wind noise. The reasons are that low-frequency sound sources are difficult to localise. Also, in wind tunnel tests, the affected components cannot be easily stiffened from outside the vehicle without impacting on the vehicle's aerodynamics. And the components are often hard to access from the inside. Lengthy testing times in the acoustic wind tunnel are the consequence. According to the current state of knowledge, this can provide a qualitative indication as to the aeroacoustic relevance of the component concerned in the early product creation phase so that appropriate countermeasures can be implemented in the event of a failure. The aim is to identify measures to optimise the entire vehicle body in terms of interior acoustics which will prevent this kind of component vibration from occurring in the first place or minimise them in an intelligent way.

However, the present results needs to be investigated further, by performing the laser dopper vibrometry results in the wind tunnel on different parts of the car to visulaise the delfection shapes of different parts of the car. It is also necessary to understand the flow visualisation behind the car to understand the wake and evaluate different methods to control the wake. The wind noise generated by wake flapping, from underbody and the wheel housing needs to investigated for a better understanding of the different sound sources.

# Bibliography


[1] Roditcheva. O, Harling. P, Sebben.S, Löfdahl.L, “Localisation of exterior and interior sound sources generated by turbulent flow around the Volvo V70.”

[2] Verrecas B, Oettle N and McQueen A, “The application of spherical beamforming techniques to localise aero-acoustic sound sources in the vehicle cabin.”

[3] Fahy. F, “Sound and structural vibration : Radiation, Transmission and Response”, 2007.

[4] Juis. C.D, Putra A “On a Simple Technique to Measure the Airborne Noise in a Motor Vehicle using Source Substitution”,2011.

[5] Putra.A Phd thesis (2008)

[6] William B. Coney, Jen Y. Her, Keith Tomaszewicz, Kevin Y. Zhang, James A. Moore, SAE TECHNICAL PAPER SERIES, “Experimental Evaluation of Wind Noise Sources: A Case Study”, 1999.

[7] Gabriella Cerrato, Sound Answers, Inc., Troy, Michigan, “Automotive Sound Quality – Powertrain, Road and Wind Noise.”

[8] “Chapter 19 : Doppler effect, United States Naval Academy.”

[9] Carsten Hoever, Scholz. M, Vibration Measurements using the Polytec Scanning Laser Doppler Vibrometer- Part 1: Theory, Division of Applied Acoustics, Chalmers University of Technology, 2013.

[10] Bernard Ginn and Karim Haddad, Brüel and Kjær “Noise Source Identification Techniques: Simple to Advanced Applications.”

[11] Christensen. J.J and Hald. J, “Brüel and Kjær Technical Review”, 2004.

[12] Lucille Lamotte, Alain Schmitt, Filip Deblauwe, “Improving Equivalent Source Distribution results in noise source localization in the space using beamforming combined with the SRTF from spherical array”, 2010.

[13] Masami Sato and Takaya Kobayashi, "A fundamental study of the flow past a circular cylinder using Abaqus/CFD", 2012.

[14] Andreas Businger, "Calculating Aerodynamically Induced Component Vibration on Motor Vehicles."